

双能量CT碘图定量参数联合形态学征象预测甲状腺微小乳头状癌颈部中央区淋巴结转移的价值

Value of the quantitative parameters of dual-energy CT iodine map combined with morphological signs in predicting the cervical central lymph node metastasis of papillary thyroid microcarcinoma

Meng Yanfei, Fei Yong, Wang Na, Wu Huajie, Liu Hongli, Fei Jimin

引用本文：

孟艳飞, 飞勇, 王娜, 等. 双能量CT碘图定量参数联合形态学征象预测甲状腺微小乳头状癌颈部中央区淋巴结转移的价值[J]. 国际放射医学核医学杂志, 2022, 46(10): 599–605. DOI: 10.3760/cma.j.cn121381–202109001–00222

Meng Yanfei, Fei Yong, Wang Na, et al. Value of the quantitative parameters of dual-energy CT iodine map combined with morphological signs in predicting the cervical central lymph node metastasis of papillary thyroid microcarcinoma[J]. International Journal of Radiation Medicine and Nuclear Medicine, 2022, 46(10): 599–605. DOI: 10.3760/cma.j.cn121381–202109001–00222

在线阅读 View online: <https://doi.org/10.3760/cma.j.cn121381–202109001–00222>

您可能感兴趣的其他文章

Articles you may be interested in

BRAF^{V600E} 突变与甲状腺乳头状癌淋巴结转移的关系及对放射性碘治疗后s-Tg的影响

The association between BRAF^{V600E} mutation and lymph node metastasis of papillary thyroid cancer and its effect on stimulated thyroglobulin radioactive iodine

国际放射医学核医学杂志. 2020, 44(11): 679–684 <https://doi.org/10.3760/cma.j.cn121381–201908003–00102>

SPECT/CT在cN0期甲状腺乳头状癌前哨淋巴结定位中的应用价值

Assessment of SPECT/CT in sentinel lymph node location in cN0 papillary thyroid carcinoma

国际放射医学核医学杂志. 2020, 44(1): 45–51 <https://doi.org/10.3760/cma.j.issn.1673–4114.2020.01.010>

¹⁸F-FDG PET/CT代谢参数在预测非小细胞肺癌患者纵隔淋巴结转移中的临床价值

Clinical value of ¹⁸F-FDG PET/CT metabolic parameters in the prediction of mediastinal lymph node metastasis in patients with non-small cell lung cancer

国际放射医学核医学杂志. 2021, 45(8): 495–500 <https://doi.org/10.3760/cma.j.cn121381–202105026–00090>

甲状腺微小乳头状癌与乳头状非微小癌的临床特点及¹³¹I疗效的比较研究

Clinical characteristics and ¹³¹I efficacy of papillary thyroid microcarcinoma and papillary thyroid non-micro carcinoma

国际放射医学核医学杂志. 2018, 42(2): 111–114, 153 <https://doi.org/10.3760/cma.j.issn.1673–4114.2018.02.003>

¹⁸F-FDG PET/CT检测淋巴结转移性鳞癌原发灶的价值

The value of ¹⁸F-FDG PET/CT imaging in detecting the primary foci of lymph node metastatic squamous cell carcinoma

国际放射医学核医学杂志. 2021, 45(9): 570–575 <https://doi.org/10.3760/cma.j.cn121381–202103028–00092>

¹⁸F-FDG PET/CT对非小细胞肺癌纵隔淋巴结转移诊断价值的Meta分析

Diagnostic value of ¹⁸F-FDG PET/CT in the diagnosis of mediastinal lymph node metastasis in non-small cell lung cancer: a Meta-analysis

国际放射医学核医学杂志. 2018, 42(1): 53–57 <https://doi.org/10.3760/cma.j.issn.1673–4114.2018.01.010>

·临床研究·

双能量CT碘图定量参数联合形态学征象预测甲状腺微小乳头状癌颈部中央区淋巴结转移的价值

孟艳飞¹ 飞勇² 王娜² 吴华杰¹ 刘红莉¹ 费继敏¹

¹ 昆明医科大学第三附属医院云南省肿瘤医院头颈外二科, 昆明 650118; ² 昆明医科大学第三附属医院云南省肿瘤医院放射科, 昆明 650118

通信作者: 费继敏, Email: jiminfei2015@163.com

【摘要】目的 探讨双能量CT碘图定量参数联合形态学征象预测甲状腺微小乳头状癌(PTMC)颈部中央区淋巴结转移(CLNM)的价值。**方法** 回顾性分析2020年1至12月就诊于昆明医科大学第三附属医院云南省肿瘤医院的经术后组织病理学检查诊断为PTMC且行中央区淋巴结清扫的165例患者的临床资料和影像资料, 其中, 男性51例、女性114例, 年龄22~69(47.8±13.9)岁, 根据组织病理学检查结果将患者分为CLNM组和无CLNM组。对病灶进行形态学征象评价, 包括多发病灶、病灶长径、形态不规则、微钙化、甲状腺边缘接触、增强扫描后边界模糊。测量术前行双能量CT扫描动、静脉期PTMC病灶的碘浓度(IC)及CT值, 计算动、静脉期病灶的标准化碘浓度(NIC)和标准化CT值(NCT值)。采用独立样本t检验比较CLNM组与无CLNM组患者动、静脉期病灶的IC、NIC以及CT值、NCT值间的差异; 采用χ²检验比较CLNM组与无CLNM组患者病灶的形态学征象。绘制单因素分析中差异有统计学意义的形态学征象及双能量CT碘图定量参数的受试者工作特征(ROC)曲线, 计算曲线下面积(AUC), 并采用二元逐步Logistic回归得到双能量CT碘图定量参数与形态学征象的联合预测系数。**结果** 形态学征象方面, CLNM组与无CLNM组患者在多发病灶、病灶长径、形态不规则、甲状腺边缘接触间的差异均有统计学意义($\chi^2=7.298\sim12.422$, 均 $P<0.01$), 且甲状腺边缘接触诊断颈部CLNM的效能最高(AUC=0.695)。双能量CT碘图定量参数方面, CLNM组患者原发灶动、静脉期的NIC和NCT值均高于无CLNM组, 且差异有统计学意义(0.36±0.02对0.32±0.03、0.70±0.11对0.59±0.10、0.43±0.06对0.37±0.07、0.81±0.08对0.75±0.12, $t=4.248\sim8.301$, 均 $P<0.01$)。且动脉期NIC诊断颈部CLNM的效能最高(AUC=0.822), 最佳临界值为0.36。双能量CT碘图定量参数联合形态学征象诊断颈部CLNM的效能最高, AUC=0.908, 灵敏度为86.70%、特异度为75.10%。甲状腺边缘接触是颈部CLNM的独立危险因素。**结论** 双能量CT碘图定量参数联合形态学征象对术前预测PTMC颈部CLNM具有重要的临床价值。

【关键词】 甲状腺肿瘤; 体层摄影术, X线计算机; 碘图; 微小乳头状癌; 中央区淋巴结转移

基金项目: 云南省卫生计生委高层次卫生技术人才培养项目(D-201659)

DOI: [10.3760/cma.j.cn121381-202109001-00222](https://doi.org/10.3760/cma.j.cn121381-202109001-00222)

Value of the quantitative parameters of dual-energy CT iodine map combined with morphological signs in predicting the cervical central lymph node metastasis of papillary thyroid microcarcinoma

Meng Yanfei¹, Fei Yong², Wang Na², Wu Huajie¹, Liu Hongli¹, Fei Jimin¹

¹the Second Department of Head and Neck Surgery, Yunnan Cancer Hospital & the Third Affiliated Hospital of Kunming Medical University, Kunming 650118, China; ²Department of Radiology, Yunnan Cancer Hospital & the Third Affiliated Hospital of Kunming Medical University, Kunming 650118, China

Corresponding author: Fei Jimin, Email: jiminfei2015@163.com

[Abstract] **Objective** To explore the value of the quantitative parameters of dual-energy CT iodine map combined with morphological signs in predicting cervical central lymph node metastasis (CLNM) in papillary thyroid microcarcinoma (PTMC). **Methods** Clinical and imaging data of 165 patients with PTMC diagnosed by postoperative histopathology and who underwent central lymph node dissection in Yunnan Cancer Hospital, the Third Affiliated Hospital of Kunming Medical University from January 2020 to December 2020 were retrospectively analyzed. The cohort included 51 males and 114 females, aged 22–69 (47.8±13.9) years old. The patients were divided into the CLNM and non-CLNM groups according to the histopathological results. Morphological signs of the lesions, including multiple lesions, long diameter, irregular shape, microcalcification, thyroid edge contact, and blurred boundary after enhanced scanning, were evaluated. The iodine concentration (IC) and CT value of the PTMC lesions in the arteriovenous phase were measured by dual-energy CT scanning before the operation. The normalized IC (NIC) and normalized CT (NCT) value of the lesions in the arteriovenous phase were calculated. Independent sample *t*-test was used to compare the IC, NIC, CT, and NCT values of the arteriovenous lesions between the two groups. χ^2 test was used to compare the morphological signs of lesions between the two groups. A receiver operator characteristic curve (ROC) was drawn for the morphological signs and quantitative parameters of the dual-energy CT iodine map with statistically significant differences in univariate analysis, and the area under curve (AUC) was calculated. Binary stepwise logistic regression was used to obtain the joint prediction coefficient of the quantitative parameters and the morphological signs. **Results** Significant differences were found in the multiple lesions, lesion diameter, irregular shape, and thyroid edge contact between the two groups ($\chi^2=7.298\sim12.422$, all $P<0.01$), and thyroid edge contact had the highest diagnostic efficiency for cervical CLNM (AUC=0.695). The NIC and NCT values of the CLNM group were higher than those of the non-CLNM group in the arteriovenous phase, and the differences were statistically significant (0.36 ± 0.02 vs. 0.32 ± 0.03 , 0.70 ± 0.11 vs. 0.59 ± 0.10 , 0.43 ± 0.06 vs. 0.37 ± 0.07 , 0.81 ± 0.08 vs. 0.75 ± 0.12 ; $t=4.248\sim8.301$, all $P<0.01$). The NIC in the arterial phase had the highest diagnostic efficiency for cervical CLNM (AUC=0.822), and the optimal cut-off value was 0.36. The quantitative parameters of the dual-energy CT iodine map combined with the morphological signs had the highest diagnostic efficiency for cervical CLNM, with AUC of 0.908, sensitivity of 86.70%, and specificity of 75.10%. Thyroid edge contact was an independent risk factor for cervical CLNM. **Conclusion** The quantitative parameters of dual-energy CT iodine map combined with the morphological signs exhibited important clinical value in predicting cervical CLNM of patients with PTMC before an operation.

[Key words] Thyroid neoplasms; Tomography, X-ray computed; Iodine map; Papillary microcarcinoma; Central lymph node metastasis

Fund program: Yunnan Provincial Health and Family Planning Commission High-level Health Technical Personnel Training Project (D-201659)

DOI: [10.3760/cma.j.cn121381-202109001-00222](https://doi.org/10.3760/cma.j.cn121381-202109001-00222)

甲状腺癌是头颈部最常见的恶性肿瘤，近年来发病率骤增，新增病例中超过50%为肿瘤长径≤10 mm的甲状腺微小乳头状癌(papillary thyroid microcarcinoma, PTMC)^[1]。PTMC早期易发生中央区淋巴结转移(central lymph node metastasis, CLNM)，转移率高达17.8%~54.1%^[2]，淋巴结转移是PTMC临床局部复发的重要危险因素^[3]。但是，对于cN0期PTMC患者是否需要行预防性中央区淋

巴结清扫(prophylactic central lymph node dissection, p-CND)仍存在争议。p-CND可导致患者喉返神经损伤、永久性甲状旁腺功能减退等并发症的风险大大增加，从而导致患者终生的生活质量下降。由于中央区淋巴结的位置较深，超声对其的诊断灵敏度仅为23%~38%^[4]，故提高影像学检查评估CLNM的准确率有助于外科医师为患者制定合理的手术方案并进行预后评估。目前，大多数研究以测量中央

区淋巴结的双能量CT定量参数来预测CLNM^[5-7],但通过PTMC原发灶的双能量CT定量参数联合形态学征象评估CLNM的研究报道甚少。本研究旨在分析cN0期PTMC原发灶的双能量CT碘图定量参数和形态学征象与CLNM的关系,探讨2者联合诊断对CLNM的预测价值。

1 资料与方法

1.1 临床资料

回顾性分析2020年1至12月就诊于昆明医科大学第三附属医院云南省肿瘤医院的165例PTMC患者的临床资料和影像资料,其中男性51例、女性114例,年龄22~69(47.8±13.9)岁。纳入标准:(1)经组织病理学检查确诊为PTMC且分期为cN0期;(2)首次行手术治疗,包括单侧甲状腺及峡部切除术和p-CND、甲状腺全切手术和p-CND、甲状腺癌根治术;(3)术前行颈部双能量CT扫描且临床和影像资料完整。排除标准:(1)经组织病理学检查确定病灶长径>10 mm;(2)双能量CT图像中病灶显示不清。以组织病理学检查结果为“金标准”,将患者分为CLNM组和无CLNM组。所有患者术前及检查前均签署了知情同意书。本研究符合《赫尔辛基宣言》的原则。

1.2 显像方法

使用德国西门子公司第三代双源CT(SOMATOM Definition Force)对患者颈部行平扫和双期增强扫描。扫描范围自主动脉弓至颅底,足向头方向。扫描参数:开启CARE Dose 4D模式,管电压A/B:80 kV/Sn150 kV,管电流A/B:190 mA/95 mA,螺距0.7 mm,层厚0.75 mm,层距0.5 mm,准直128 mm×0.6 mm,机架旋转时间250 ms。对比剂使用碘普罗胺(德国拜耳公司,370 mgI/ml),剂量1.0 ml/kg,注射流速3 ml/s,随后注射0.9%氯化钠溶液(中国大家制药有限公司)30 ml。采用团注对比剂跟踪技术,监测平面为主动脉弓,触发阈值100 HU,延迟5 s扫描动脉期,动脉期后延迟25 s扫描静脉期。

1.3 形态学征象评价

对病灶进行形态学征象评价,包括多发病灶(病灶数目>1,根据组织病理学检查结果定位病灶)、病灶长径(多发病灶取最大病灶的长径)、形态不规则(除圆形、类圆形外的形态)、微钙化(长径<

2 mm的沙砾样钙化)、甲状腺边缘接触(CT平扫时正常高密度的甲状腺边缘被低密度的病灶占据,边缘连续性中断,且病灶长径位于甲状腺边缘)、增强扫描后边界模糊(增强扫描后病灶与甲状腺间的密度差小于相应的平扫密度差)。由1名放射科副主任医师和1名具有10年以上工作经验的放射科主治医师共同完成阅片,意见不一致时共同商议确定。

1.4 碘浓度 (iodine concentration, IC) 和标准化碘浓度 (normalized iodine concentration, NIC) 的测量

使用德国西门子公司后处理工作站(Syngo.via)进行IC和NIC测量,启动Dual-Energy程序,选择Liver VNC处理模式获取碘图。由1名具有10年以上工作经验的放射科主治医师分别在动、静脉期测量碘图中ROI的IC和CT值,取ROI面积>70%的病灶实质成分,连续取3个典型层面后得到平均值,最大程度避开钙化、坏死及伪影区。为减少个体差异,以同时相的颈内动脉IC和CT值作为对照,计算NIC和标准化CT(normalized CT, NCT)值,NIC为ROI的IC与同时相颈内动脉IC的比值,NCT值为ROI的CT值与同时相颈内动脉CT值的比值。

1.5 统计学方法

应用SPSS 23.0软件对数据进行统计学分析。符合正态分布的计量资料以 $\bar{x}\pm s$ 表示,采用独立样本t检验(方差齐)比较CLNM组与无CLNM组患者动、静脉期病灶的IC、NIC以及CT值、NCT值;采用 χ^2 检验比较CLNM组与无CLNM组患者病灶的形态学征象。绘制单因素分析中差异有统计学意义的形态学征象及双能量CT碘图定量参数的ROC曲线,计算AUC,并采用二元逐步Logistic回归得到双能量CT碘图定量参数与形态学征象的联合预测系数。 $P<0.05$ 为差异有统计学意义。

2 结果

2.1 一般资料

165例PTMC患者中有79例发生CLNM,其中男性32例、女性47例,年龄22~69(44.9±13.3)岁,即为CLNM组;有86例患者未发生CLNM,其中男性19例、女性67例,年龄24~67(50.4±14.1)岁,即为无CLNM组。

2.2 原发灶形态学征象的比较

由表1可知,2组患者在多发病灶、病灶长径、形态不规则、甲状腺边缘接触间的差异均有统计学意义(均 $P<0.01$),而在微钙化、增强扫描后边界模糊间的差异均无统计学意义(均 $P>0.05$)。典型原发灶的形态学征象见图1A、B。

2.3 原发灶动、静脉期双能量CT碘图定量参数的比较

由表2可知,2组患者原发灶动、静脉期的IC、CT值间的差异均无统计学意义(均 $P>0.05$);而CLNM组患者原发灶动、静脉期的NIC和NCT值均高于无CLNM组,且差异均有统计学意

表1 165例甲状腺微小乳头状癌患者原发灶CT形态学征象的比较(例)

Table 1 Comparison of CT morphological features of primary lesions in 165 patients with papillary thyroid microcarcinoma (case)

组别	多发病灶		病灶长径		微钙化		增强扫描后边界模糊		形态不规则		甲状腺边缘接触	
	有	无	≤5 mm	>5 mm	有	无	有	无	有	无	有	无
CLNM组($n=79$)	49	30	28	51	26	53	21	58	46	33	52	27
无CLNM组($n=86$)	32	54	49	37	23	63	29	57	32	54	33	53
χ^2 值	10.146		7.671		0.750		0.994		7.298		12.422	
P值	0.001		0.006		0.386		0.319		0.007		<0.001	

注:CT为计算机体层摄影术;CLNM为中央区淋巴结转移

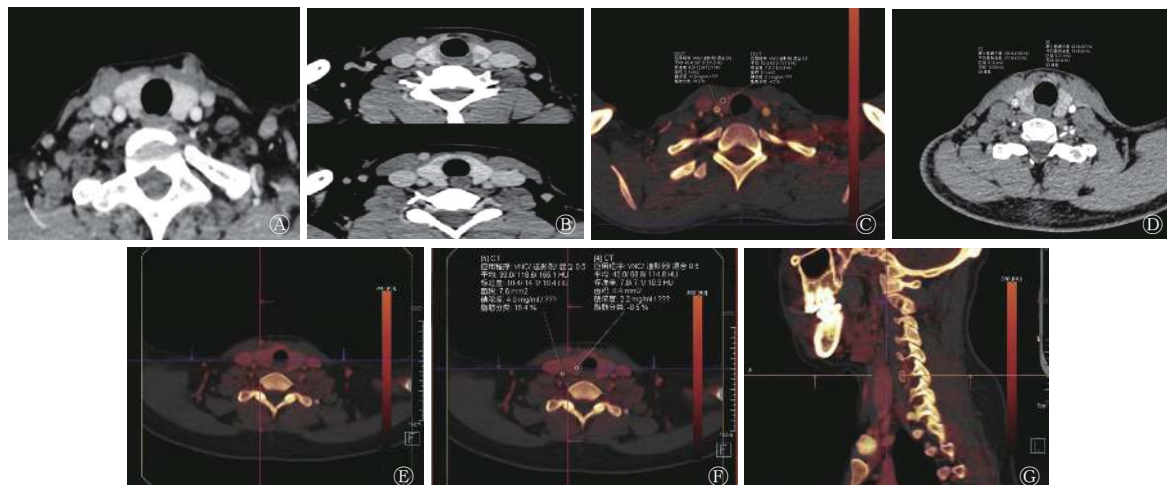


图1 甲状腺微小乳头状癌患者典型原发灶的CT形态学征象(A~B)、双能量CT动脉期IC和CT值的测量(C~D)以及双能量CT碘图(E~G)。A为男性患者(46岁),显示病灶呈甲状腺边缘接触,且形态不规则;B为女性患者(51岁),上图、下图分别显示甲状腺腺体内左侧中部、右侧上部均可见病灶;C为女性患者(31岁)的双能量CT动脉期IC测量图,NIC为0.39;D为女性患者(58岁)的双能量CT动脉期CT值测量图,NCT值为0.46;E~G为女性患者(38岁)的双能量CT碘图,显示甲状腺右叶病灶,右侧中央区转移性淋巴结。CT为计算机体层摄影术;IC为碘浓度;NIC为标准化碘浓度;NCT值为标准化CT值

Figure 1 Typical CT morphological features of primary lesions (A~B), measurement of IC and CT values in arterial phase (C~D), and dual-energy CT iodine map (E~G) in patients with thyroid papillary microcarcinoma

表2 165例甲状腺微小乳头状癌患者原发灶动、静脉期双能量CT碘图定量参数的比较($\bar{x}\pm s$)

Table 2 Comparison of quantitative parameters of dual-energy CT iodine map of primary lesions at arterial and venous stages in 165 patients with papillary thyroid microcarcinoma ($\bar{x}\pm s$)

组别	IC(mg/ml)		NIC		CT值(HU)		NCT值	
	动脉期	静脉期	动脉期	静脉期	动脉期	静脉期	动脉期	静脉期
CLNM组($n=79$)	3.78±0.88	3.29±1.15	0.36±0.02	0.70±0.11	94.42±36.23	60.06±21.57	0.43±0.06	0.81±0.08
无CLNM组($n=86$)	3.59±0.93	2.98±0.86	0.32±0.03	0.59±0.10	85.04±34.08	57.82±18.49	0.37±0.07	0.75±0.12
t 值	1.362	1.890	8.301	6.241	1.713	0.718	5.592	4.248
P值	0.175	0.610	<0.01	<0.01	0.089	0.474	<0.01	<0.01

注:CT为计算机体层摄影术;CLNM为中央区淋巴结转移;IC为碘浓度;NIC为标准化碘浓度;NCT值为标准化CT值

义(均 $P<0.01$)。PTMC 患者病灶动脉期 IC、CT 值的测量见图 1C、D, 双能量 CT 碘图见图 1E~G。

2.4 原发灶形态学征象、双能量 CT 碘图定量参数及两者联合诊断 CLNM 的效能

由表 3、图 2 可知, 双能量 CT 碘图定量参数

表 3 CT 形态学征象、双能量 CT 碘图定量参数及两者联合诊断甲状腺微小乳头状癌中央区淋巴结转移的效能

Table 3 CT morphological features, quantitative parameters of dual-energy CT iodine map of primary lesions, and their combined efficacy in diagnosing central lymph node metastasis in papillary thyroid microcarcinoma

诊断指标	灵敏度 (%)	特异度 (%)	AUC
动脉期NIC	68.00	90.00	0.822
静脉期NIC	56.00	83.00	0.748
动脉期NCT值	65.00	71.00	0.723
静脉期NCT值	71.00	52.00	0.653
双能量CT碘图定量参数	79.20	86.00	0.829
多发病灶	76.40	58.10	0.625
病灶长径	71.20	69.20	0.586
形态不规则	68.40	45.60	0.564
甲状腺边缘接触	81.30	49.20	0.695
CT形态学征象	74.20	69.50	0.716
双能量CT碘图定量参数+CT形态学征象	86.70	75.10	0.908

注: CT 为计算机体层摄影术; NIC 为标准化碘浓度; NCT 值为标准化 CT 值; AUC 为曲线下面积

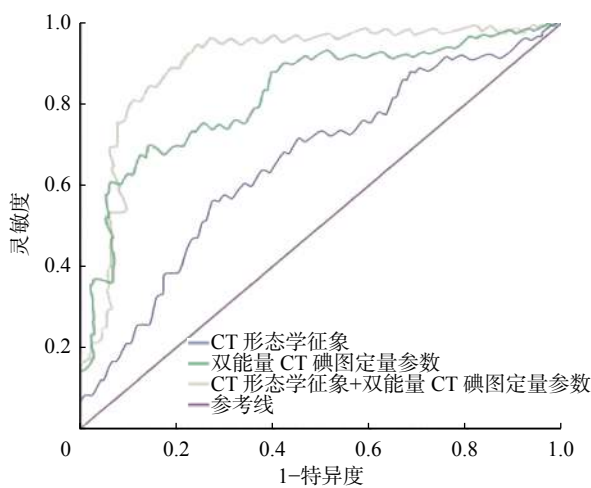


图 2 CT 形态学征象、双能量 CT 碘图定量参数及两者联合诊断甲状腺微小乳头状癌中央区淋巴结转移的受试者工作特征曲线 CT 为计算机体层摄影术

Figure 2 Receiver operator characteristic curves of CT morphological features, quantitative parameters of dual-energy CT iodine map of primary focus, and their combined efficacy in diagnosing central lymph node metastasis in papillary thyroid microcarcinoma

中, 动、静脉期 NIC 对 CLNM 的诊断效能较动、静脉期 NCT 值更高, 其中, 动脉期 NIC 的诊断效能最高($AUC=0.822$), 且特异度最高(90.00%), 其最佳临界值为 0.36; 静脉期 NIC 的诊断效能、灵敏度、特异度均较动脉期 NIC 低。形态学征象中, 甲状腺边缘接触对 CLNM 的诊断效能最高($AUC=0.695$), 且灵敏度最高(81.30%)。相比于单独采用双能量 CT 碘图定量参数或形态学征象对 CLNM 进行诊断, 两者联合的诊断效能最高($AUC=0.908$), 灵敏度为 86.70%, 特异度为 75.10%。

2.5 原发灶形态学征象及双能量 CT 碘图定量参数与 CLNM 的多因素分析

二元逐步 Logistic 回归分析结果显示, 甲状腺边缘接触是 CLNM 的独立危险因素, B 值=1.129, 标准误为 0.325, Wald χ^2 值=12.093, OR 值=3.093, 95%CI: 1.637~5.845, $P=0.001$ 。

3 讨论

2015 版美国甲状腺学会制定的成年人甲状腺结节与分化型甲状腺癌诊治指南^[8]表明, 外科医师的术式选择以及对患者预后的评估依赖于术前明确淋巴结是否转移。由于大多数 PTMC 患者没有典型的临床症状, 术前诊断主要依赖于影像表现。超声对 PTMC 颈部 CLNM 的诊断准确率受气管和胸骨伪影等的影响, 而 CT 对 CLNM 的诊断更为客观, 且不受气管和胸骨影响, 在一定程度上其诊断效能高于超声。金弋人等^[9]的研究结果表明, 中央区淋巴结的 IC 联合形态学征象预测 CLNM 具有一定的参考价值, 但仍无法避免中央区淋巴结定位困难和漏诊的问题。因此, 本研究旨在从 PTMC 原发灶角度出发, 探究双能量 CT 碘图定量参数联合形态学征象对 CLNM 的诊断效能, 为预测 cN0 期 PTMC 患者 CLNM 提供新的依据。

我们通过对比 CLNM 组和无 CLNM 组患者的 CT 形态征象, 发现 CLNM 与多发病灶、病灶长径、形态不规则、甲状腺边缘接触有关, 这与既往研究^[10-14]报道一致。本研究结果显示, 多发病灶较单发病灶更易发生 CLNM, 分析原因, 可能是多发病灶导致 PTMC 发生在甲状腺边缘的概率升高^[15], 且肿瘤组织更易在甲状腺内播散。本研究以病灶长径 5 mm 为界限, 发现长径 >5 mm 的 PTMC 原发灶发生 CLNM 的概率较高。Luo 等^[16]

报道,长径>5 mm的PTMC原发灶是CLNM的独立危险因素,且随着病灶长径的增大,发生CLNM的概率升高。李宁等^[17]报道,原发灶有甲状腺边缘接触的患者CLNM阳性的优势比是无边缘接触的3.165倍,这提示甲状腺边缘接触可作为诊断CLNM的重要形态征象。本研究的多因素分析结果表明,甲状腺边缘接触是CLNM的独立危险因素。Xiang等^[18]的研究结果显示,超声提示甲状腺包膜侵犯可能是由于病灶突破了包膜并浸润包膜内的淋巴管。我们认为甲状腺边缘接触与其有共同的组织学基础,两者均表现为病灶边界与甲状腺包膜之间有较大的接触面积。当PTMC原发灶形态不规则时,更易发生颈部CLNM,这可能是由肿瘤通过调整自身的形态,突破肿瘤包膜来与甲状腺包膜上丰富的淋巴网接触造成的。

双能量CT图像经后处理得到的碘图可直观显示病灶中碘含量的差别,从而间接反映病灶中的血液供应情况,进一步提高了其对CLNM的诊断效能^[19]。Lai等^[20]发现,新生的血管和肿瘤的恶性程度与淋巴结转移密切相关,肿瘤内的血管生长因子能有效促进病灶毛细血管和淋巴管的生成,从而发生转移。甲状腺癌病灶和转移的淋巴结均具有摄碘与血流丰富的特征^[21]。本研究以同时相颈内动脉的IC、CT值为参考,结果显示,CLNM组患者动、静脉期的NIC、NCT值均高于无CLNM组,动脉期NIC、NCT值的诊断效能均高于静脉期,且动脉期NIC的诊断效能最高、最佳临界值为0.36、特异度达90.00%,这与肿瘤动脉期新生的微血管增多、血流速度增快、增强扫描早期即明显强化、摄碘率增高,即呈“快进快出”的强化模式相关;而静脉期肿瘤的碘含量呈平台期改变,因此,测量动脉期IC具有更高的诊断效能。同样,Park等^[22]的研究结果表明,动脉期CT较延迟期CT对甲状腺乳头状癌颈部淋巴结转移的诊断准确率更高。此外,本研究中,动脉期NIC的诊断效能高于NCT值。碘图可以有效消减颈部伪影并抑制背景CT值,对IC更加敏感,更能准确地体现病灶的碘分布和血供的差异。本研究结果显示,双能量CT碘图定量参数联合形态学征象诊断CLNM的效能较单一方法更高,灵敏度为86.70%,特异度为75.10%。本研究中cN0期PTMC患者术后CLNM率高达48%,因此,通过术前双能量CT碘

图定量参数联合形态学征象预测CLNM,能够帮助外科医师制定合理手术方案,从而使更多的患者获益。

本研究还存在以下局限性:(1)本研究为单中心研究且纳入的病例数有限,有待进一步开展多中心、大样本量的深入研究;(2)只测量了双能量CT碘图定量参数,后续可增加能谱曲线、影像组学等为术前预测PTMC颈部CLNM提供更多有价值的信息。

综上所述,甲状腺边缘接触是PTMC颈部CLNM的独立危险因素,双能量CT碘图定量参数联合形态学征象对术前预测PTMC颈部CLNM有重要的临床价值,可为cN0期PTMC患者行p-CND提供新依据。

利益冲突 所有作者声明无利益冲突

作者贡献声明 孟艳飞负责文献的查阅、数据的统计、论文的撰写;飞勇负责命题的提出与设计、影像结果的判读;王娜负责图像的采集与处理;吴华杰负责临床数据的整理与分析;刘红莉负责数据的分析;费继敏负责论文的指导与审阅

参 考 文 献

- [1] Olson E, Wintheiser G, Wolfe KM, et al. Epidemiology of thyroid cancer: a review of the national cancer database, 2000–2013[J/OL]. Cureus, 2019, 11(2): e4127[2021-8-31]. <https://www.cureus.com/articles/15462-epidemiology-of-thyroid-cancer-a-review-of-the-national-cancer-database-2000-2013>. DOI: 10.7759/cureus.4127.
- [2] Xu YN, Xu L, Wang JD. Clinical predictors of lymph node metastasis and survival rate in papillary thyroid microcarcinoma: analysis of 3607 patients at a single institution[J]. J Surg Res, 2018, 221: 128–134. DOI: 10.1016/j.jss.2017.08.007.
- [3] Pérez-Soto RH, Velázquez-Fernández D, Arellano-Gutiérrez G, et al. Preoperative and postoperative risk stratification of thyroid papillary microcarcinoma: a comparative study between Kuma criteria and 2015 American Thyroid Association guidelines risk stratification[J]. Thyroid, 2020, 30(6): 857–862. DOI: 10.1089/thy.2019.0698.
- [4] Zhao HQ, Li HH. Meta-analysis of ultrasound for cervical lymph nodes in papillary thyroid cancer: diagnosis of central and lateral compartment nodal metastases[J]. Eur J Radiol, 2019, 112: 14–21. DOI: 10.1016/j.ejrad.2019.01.006.
- [5] 郑凌琳,田扬,赵卫,等.双能CT诊断颈部中央区甲状腺乳头状癌小淋巴结转移[J].中国医学影像技术,2017,33(6):863–867. DOI: 10.13929/j.1003-3289.201607025.
- Zheng LL, Tian Y, Zhao W, et al. Dual energy CT in diagnosis of central cervical metastatic lymph nodes in patients with papillary thyroid cancer[J]. Chin J Med Imaging Technol, 2017, 33(6): 863–867. DOI: 10.13929/j.1003-3289.201607025.

- [6] 何慕真, 马明平, 林阳, 等. 双能量CT成像在诊断甲状腺乳头状癌颈部淋巴结转移中的临床应用价值[J]. 中国癌症杂志, 2018, 28(7): 497–504. DOI: 10.19401/j.cnki.1007-3639.2018.07.004.
- He MZ, Ma MP, Lin Y, et al. Diagnostic value of dual-energy CT imaging for cervical lymph nodes metastasis in the patients with papillary thyroid cancer[J]. China Oncol, 2018, 28(7): 497–504. DOI: 10.19401/j.cnki.1007-3639.2018.07.004.
- [7] Zhuo SQ, Sun JY, Chang JY, et al. Dual-source dual-energy thin-section CT combined with small field of view technique for small lymph node in thyroid cancer: a retrospective diagnostic study[J]. Gland Surg, 2021, 10(4): 1347–1358. DOI: 10.21037/gs-20-822.
- [8] Haugen BR, Alexander EK, Bible KC, et al. 2015 American Thyroid Association management guidelines for adult patients with thyroid nodules and differentiated thyroid cancer: the American Thyroid Association guidelines task force on thyroid nodules and differentiated thyroid cancer[J]. Thyroid, 2016, 26(1): 1–133. DOI: 10.1089/thy.2015.0020.
- [9] 金弋人, 韩丹, 蒋悦, 等. 双能量CT增强碘浓度结合形态学在诊断甲状腺乳头状癌中央组淋巴结转移的价值[J]. 临床放射学杂志, 2018, 37(3): 391–395. DOI: 10.13437/j.cnki.jcr.2018.03.008.
- Jin YR, Han D, Jiang Y, et al. Iodine concentration on dual-energy contrast enhanced CT in differential diagnosis of the metastatic central lymph nodes in patients with papillary thyroid cancer[J]. J Clin Radiol, 2018, 37(3): 391–395. DOI: 10.13437/j.cnki.jcr.2018.03.008.
- [10] Song JL, Yan T, Qiu WW, et al. Clinical analysis of risk factors for cervical lymph node metastasis in papillary thyroid microcarcinoma: a retrospective study of 3686 patients[J/OL]. Cancer Manag Res, 2020, 12: 2523–2530[2021-08-31]. <https://www.dovepress.com/clinical-analysis-of-risk-factors-for-cervical-lymph-node-metastasis-i-peer-reviewed-fulltext-article-CMAR>. DOI: 10.2147/CMAR.S250163.
- [11] Zhang C, Li BJ, Liu Z, et al. Predicting the factors associated with central lymph node metastasis in clinical node-negative (cN0) papillary thyroid microcarcinoma[J]. Eur Arch Otorhinolaryngol, 2020, 277(4): 1191–1198. DOI: 10.1007/s00405-020-05787-1.
- [12] Sheng L, Shi JY, Han B, et al. Predicting factors for central or lateral lymph node metastasis in conventional papillary thyroid microcarcinoma[J]. Am J Surg, 2020, 220(2): 334–340. DOI: 10.1016/j.amjsurg.2019.11.032.
- [13] 潘勐, 黄勇, 汪汉华, 等. CT征象联合临床病理特征对甲状腺微小乳头状癌中央组淋巴结转移的预测价值[J]. 中国普外基础与临床杂志, 2022, 29(6): 738–742. DOI: 10.7507/1007-9424.202107088.
- Pan M, Huang Y, Wang HY, et al. Prediction of lymph node metastasis in central group of thyroid papillary microcarcinoma by CT signs combined with clinicopathological features[J]. Chin J Bases Clin Gen Surg, 2022, 29(6): 738–742. DOI: 10.7507/1007-9424.202107088.
- [14] Liu WF, Wang SF, Xia XT. Risk factor analysis for central lymph node metastasis in papillary thyroid microcarcinoma [J/OL]. Int J Gen Med, 2021, 14: 9923–9929[2021-08-31]. <https://www.dovepress.com/risk-factor-analysis-for-central-lymph-node-metastasis-in-papillary-th-peer-reviewed-fulltext-article-IJGM>. DOI: 10.2147/IJGM.S346143.
- [15] 梁振威, 邵玉红, 陈蕾, 等. 多灶性甲状腺微小乳头状癌中央区淋巴结转移影响因素的研究[J]. 中国超声医学杂志, 2021, 37(9): 971–973. DOI: 10.3969/j.issn.1002-0101.2021.09.004.
- Liang ZW, Shao YH, Chen L, et al. Clinical and ultrasonic analysis of central lymph node metastasis risk factors in patients with multiple papillary thyroid microcarcinoma[J]. Chin J Ultrasound Med, 2021, 37(9): 971–973. DOI: 10.3969/j.issn.1002-0101.2021.09.004.
- [16] Luo Y, Zhao Y, Chen K, et al. Clinical analysis of cervical lymph node metastasis risk factors in patients with papillary thyroid microcarcinoma[J]. J Endocrinol Invest, 2019, 42(2): 227–236. DOI: 10.1007/s40618-018-0908-y.
- [17] 李宁, 舒艳艳, 韩志江. CT征象联合临床特征对cN0期单发甲状腺乳头状癌中央组淋巴结转移的预测价值[J]. 中国临床医学影像杂志, 2016, 27(9): 616–619.
- Li N, Shu YY, Han ZJ. Predictive value of CT combined with clinical features in diagnosing central lymph node metastasis of papillary thyroid carcinoma in stage cN0[J]. J Chin Clin Med Imaging, 2016, 27(9): 616–619.
- [18] Xiang TH, Yan WY, Zhou LA. Retrospective analysis of prognostic factors in patients of papillary thyroid microcarcinoma [J/OL]. Oncotarget, 2018, 9(85): 35553–35558[2021-08-31]. <https://www.oncotarget.com/article/26248/text>. DOI: 10.18632/oncotarget.26248.
- [19] Rizzo S, Radice D, Femia M, et al. Metastatic and non-metastatic lymph nodes: quantification and different distribution of iodine uptake assessed by dual-energy CT[J]. Eur Radiol, 2018, 28(2): 760–769. DOI: 10.1007/s00330-017-5015-5.
- [20] Lai CW, Duh QY, Chen CW, et al. VEGF-D and a preoperative serum levels predict nodal and distant metastases in differentiated thyroid cancer patients[J]. World J Surg, 2015, 39(7): 1742–1749. DOI: 10.1007/s00268-015-3016-6.
- [21] Roele ED, Timmer VCML, Vaassen LAA, et al. Dual-energy CT in head and neck imaging[J/OL]. Curr Radiol Rep, 2017, 5(5): 19[2021-08-31]. <https://link.springer.com/article/10.1007/s40134-017-0213-0>. DOI: 10.1007/s40134-017-0213-0.
- [22] Park JE, Lee JH, Ryu KH, et al. Improved diagnostic accuracy using arterial phase CT for lateral cervical lymph node metastasis from papillary thyroid cancer[J]. AJNR Am J Neuroradiol, 2017, 38(4): 782–788. DOI: 10.3174/ajnr.A5054.

(收稿日期: 2021-09-01)